Effects of elevated temperature and crude oil on the properties of a hydrogenated nitrile butadiene rubber elastomer

Long Pan, Jinzhu Tan, Xuemei Han, Peng Li, Wujian Zhang

School of Mechanical and Power Engineering, Nanjing Tech University, Nanjing 211816, China
Correspondence to: J. Z. Tan (E-mail: tjznjut@njtech.edu.cn)

ABSTRACT: The stability and durability of hydrogenated nitrile butadiene rubber (HNBR) material in crude oil environments are of great importance for petroleum equipment to resist leakage and to ensure reliability. In this paper, an HNBR material was fabricated, and the degradation of the HNBR material was investigated in simulated crude oil environments. One crude oil and three temperatures (50 °C, 75 °C, and 100 °C, based on actual crude oil operations, were used in this study. Weight changes for the HNBR specimens were monitored after exposure to the environments over time. Optical microscopy was used to show the topographical changes on the specimen surfaces. Attenuated total reflection Fourier transform infrared (ATR-FTIR) spectroscopy was employed to study the surface chemistry of the HNBR material before and after exposure to the simulated crude oil environments at selected times. Mechanical property tests (tensile and compressive stress–strain tests, tear strength test, and compression set test) were conducted to assess the changes in mechanical properties of the HNBR specimens before and after exposure to the environments. The test results show that the physical–mechanical properties of the HNBR material changed significantly. The temperature and the crude oil had a direct effect on the degradation of the mechanical properties. The ATR-FTIR test results indicate that the surface chemistry changed via chain crosslinking in the material after exposure to the environments over time. The degradation mechanisms of the HNBR material after exposure to the crude oil could be due to the presence of chain crosslinking, chain mobility, and backbone scission. © 2016 Wiley Periodicals, Inc. J. Appl. Polym. Sci. 2016, 133, 44012.

INTRODUCTION

Hydrogenated nitrile butadiene rubber (HNBR) is formed by the selective hydrogenation of the carbon–carbon unsaturation of nitrile butadiene rubber (NBR) in solution at high pressure and temperature. It is well known that HNBR has better physical strength and better retention of properties after long-term exposure to heat, oil, chemicals, and radiation[1,2] than NBR. Therefore, the HNBR material can be used as seals in many industrial applications, especially in petroleum industrial applications, such as gaskets, radial lip seals,[3] and stator material for progressing cavity pumps.[4] The use of HNBR for oil field components could extend the lifetime of the articles, thereby reducing the maintenance frequency or extending the replacement cycles for those parts.[5]

In petroleum industrial applications, more challenging oil field locations are targeted for future exploitation.[6] However, the long-term stability and durability of the seal material in crude oil environments are critical in resisting leakage and ensuring the stability and security of the equipment. The degradation of the physical and mechanical properties of the HNBR material exposed to oil environments is an important issue.[7–11] Although the HNBR material has excellent oil resistance, the oil is always absorbed by the rubber material and leads to changes in mass and dimensions of the HNBR specimens. Furthermore, the absorption of oil makes the elastic modulus and hardness of the rubber material decrease,[12] and the other mechanical properties could change.

The HNBR material used as seals is generally exposed to crude oil environments at elevated temperatures of 50–100 °C. The rubber material, which is known as an organic macromolecule elastic material, is often sensitive to temperature changes.[13–15] An elevated temperature may lead to a decrease in the mechanical properties and the antifatigue and antitear properties. Consequently, the rubber material may no longer meet the service requirements.[16,17] Therefore, elevated temperature is also a main factor that affects the properties of the rubber material.

The changes of the physical and mechanical properties of HNBR materials in hot air or in chemical environments were

Table 1. Formula of the HNBR Material in Phr

HNBR	Carbon black N330	Stearic acid	Zinc oxide	Sulfur	Accelerator TMTD	Accelerator M	Accelerator DM	Vulkanox RD	Vulkanox 4010	Total
100	50	0.5	5	0.5	1.5	0.5	1	1.5	1.5	162

examined intensively by many researchers.[18–28] For example, Cadambi and Ghassemieh[18] studied the influence of organoclay reinforcement in HNBR after subjecting it to long-term oxidative aging and immersion studies. Wang et al.[19] investigated the mechanical properties and hot-air aging resistance of hydrogenated nitrile-butadiene rubber–chloroprene rubber blends. Nasreddine et al.[20] discussed the mechanical and aging properties of ultrahigh acrylonitrile HNBR elastomers in an IRM903 fluid, fuel-alcohol blends, and biodiesel fuels. Sheng et al.[21] showed the heat-resistance property of peroxide-cured fully saturated HNBR materials with a small amount of sulfur. Alcock and Jørgensen[22] reported the mechanical properties of the typical carbon black–reinforced HNBR exposed to a mix of simulated sweet oil at elevated temperatures and pressure. Although there is substantial literature regarding the degradation of the HNBR material, few results were reported for the degradation and degradation mechanisms of HNBR materials in actual crude oil and temperature conditions.

In this work, the aging processes of the HNBR material in the simulated crude oil at various temperatures were studied. The aim was to investigate changes in physical–mechanical properties and degradation mechanisms for the HNBR specimens exposed to crude oil environments, and to understand the effects of elevated temperature and crude oil on the degradation in the exposure. The formula of the HNBR material was designed, and then the HNBR elastomeric material was fabricated. One crude oil and three temperatures (50 °C, 75 °C, and 100 °C, based on actual crude oil operations, were used in this study. Weight changes were monitored for the HNBR specimens after exposure to the crude oil environments over time. Optical microscopy was used to show the topographical changes on the surfaces of specimens. Attenuated total reflection Fourier transform infrared (ATR-FTIR) spectroscopy was employed to study the surface chemistry of the HNBR material before and after exposure to the crude oil environments at selected times. Mechanical property tests (tensile and compression stress–strain tests, tear strength test, and compression set test) were conducted to assess the changes in mechanical properties of the HNBR specimens before and after exposure to the crude oil environments.

EXPERIMENTAL

Material and Simulated Crude Oil Environment
The material used in this study is the HNBR material with the formula shown in Table 1. The basic HNBR (Zeptol2010) is a commercial material from the Zeon Corporation in Japan. The mass percentage of the acrylonitrile for the basic rubber is 36%, and the hydrogenation percentage is 95%. In order to improve the temperature and oxygen resistance, the vulkanox RD (1,2-dihydro-2,2,4-trimethyl-quinoline) and vulkanox 4010 (N-cyclohexyl-N′-phenyl-p-phenylenediamine) from Sunsine Chemical in China were added into the material together. The HNBR

material was fabricated with a cure temperature of 140 °C, a molding time of 25 min, and a molding pressure of 10 MPa.

Crude oil from Pazflor field was used in this study to age the material. Pazflor field is located in deepwater offshore Angola block 17. The crude oil has a density of 897.3 kg/m^3 measured at 20 °C, a kinematic viscosity of 13.79 mm^2/s measured at 50 °C, an acid value of 1.28 mgKOH/g, and a carbon residue rate of 4.54%. In addition, the compositions of the crude oil are listed in Table 2.

Aging Methods
Specimens from the fabricated HNBR material were prepared for the various tests in this work. The specimens were placed in metallic containers containing the crude oil mentioned above. The containers were then put in the ovens at 50 °C, 75 °C, and 100 °C for 8 weeks. The test temperatures are close to the actual temperatures of crude oil operations. Specimens were taken out at selected times for examination.

Characterization Methods
Weight Examination. To study the effects of elevated temperature and crude oil on the weight, rectangular specimens were prepared. The length, width, and thickness of the specimens for weight examinations are 25 mm, 25 mm, and 2 mm, respectively. The changes of the specimens in weight over time were monitored using an electronic microbalance. Three specimens were measured over time for each exposure environment, and the average values are shown in this paper.

Optical Microscopy and ATR-FTIR Tests. Rectangular specimens from the HNBR material were prepared. The length, width, and thickness of the specimens for optical microscopy and ATR-FTIR tests are 50 mm, 25 mm, and 2 mm, respectively. The dimensions of the specimens for ATR-FTIR tests are the same as those of the specimens for the optical microscopy tests.

The surface conditions of the specimens before and after exposure to the crude oil were examined using an optical microscope (Zeiss Axio Imager A1m OM, Germany). In addition,

Table 2. Composition of the Crude Oil

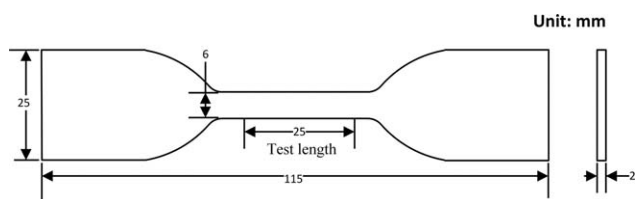| Element	Value
Carbon (%)	86.6
Hydrogen (%)	12.8
Sulfur (%)	0.4
Nitrogen (%)	0.1
Ni (ppm)	15.3
V (ppm)	6.2
Fe (ppm)	5.2
Na (ppm)	3.2
Ca (ppm)	2.2

Figure 1. Geometry and dimensions of dumbbell-type specimen for tensile stress–strain test.

ATR-FTIR spectroscopy was performed on the surface of the specimens using a Nexus Model 670 Instrument (Nicolet Instrument, USA) and ran with 32 scans at a resolution $0.1\,cm^{-1}$. The infrared radiation (IR) penetrates the surface of the test specimen to approximately 1 μm.

In order to avoid the effect of the remaining crude oil solution on the specimen surface in the ATR-FTIR results, the specimens were cleaned using experimental alcohol with a purity of 95% and a volatility of 99.9% to remove the excess crude oil on the surface and were dried at room temperature (about 25°C) before examination.

Tensile Stress–Strain Test and Tear Test. In order to study the effects of elevated temperature and crude oil on the tensile stress–strain and tear strength properties, dumbbell-shaped and trouser-shaped specimens were prepared according to ISO 37: 2005 and ISO 34-1: 2010, respectively. The geometry and dimensions for the tensile test specimens are shown in Figure 1. The geometry and dimensions for the tear test specimens are shown in Figure 2.

In order to assess the tensile and tear properties of the specimens before and after exposure to the crude oil environment, the tensile and tear tests were performed using a high- and low-temperature universal instrument (MZ4000, MingZhu Instruments Ltd in China) with a precision of force measurement of ±0.5% and a precision of displacement measurement of ±0.5%. The forces and displacements were controlled and recorded automatically by a computer. All tests for the specimens after exposure were conducted at their exposure temperatures. The specimens without exposure were also characterized at 50°C, 75°C, and 100°C for comparison. All tensile stress–strain tests were performed at the rate of 500 mm/min, and the tear tests were performed at the rate of 100 mm/min in displacement-controlled mode.

The tensile tests were performed according to ISO 37: 2005. At least three dumbbell-type specimens were removed from the crude oil solution and tested at each selected time. The middle values of the tensile test results are shown in this paper. In addition, the tear tests were performed according to ISO 34-1:
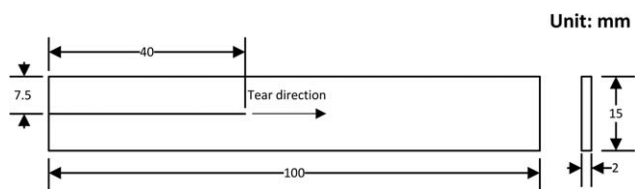

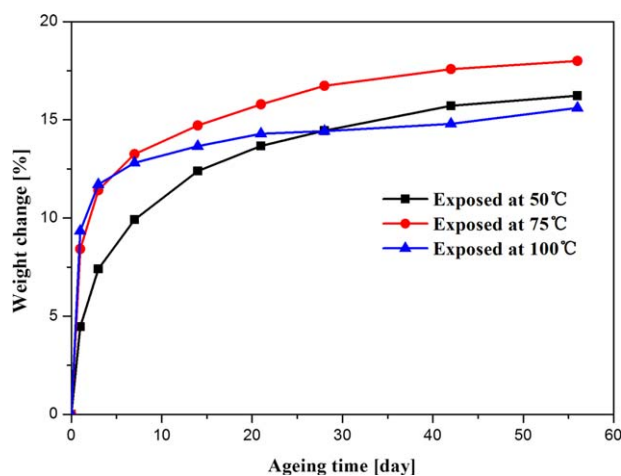**Figure 2.** Geometry and dimensions of trouser-type specimen for tear test.

Figure 3. Weight changes with exposure time for the HNBR material exposed to crude oil at 50°C, 75°C, and 100°C. [Color figure can be viewed in the online issue, which is available at wileyonlinelibrary.com.]

2010. At least five trouser-type specimens were removed from the crude oil solution and tested at each selected time, and the multipeak traces obtained in the determinations of tear strength were analyzed according to ISO 6133: 2014. The average values of the tear strength are shown in this paper.

Compression Stress–Strain Test and Compression Set Test. The specimen for the compression stress–strain test has dimensions of 13 ± 0.5 mm in diameter and 6.3 ± 0.3 mm in height. The geometry and dimensions of the specimen for the compression set test are the same as those of the specimen for the compressive stress–strain test, and the tests were performed using the same machine as for the tensile stress–strain tests.

The compression stress–strain tests were performed according to ISO 7743: 2007. Three cylindrical specimens were tested for each exposure condition, and the middle values of the compression stress–strain test results are shown in this paper. For the compression set tests, the compression period was 168 hours according to ISO 815:1991. Three specimens were tested for each exposure condition, and the average values of the compression set rate are shown in this paper.

RESULTS AND DISCUSSION

Weight Change

The specimens after exposure were removed from the crude oil at selected times. The surfaces of the specimens were carefully cleaned using experimental alcohol to remove the excess crude oil and dried at room temperature before the weight changes were monitored. The percent of weight increase, WI, was calculated using eq. (1):

$$WI = (W_2 - W_1)/W_1 \times 100 \qquad (1)$$

where W_1 is the initial weight of the specimen in air, and W_2 is the weight of the aged specimen in air.

Figure 3 shows the change of weight over time at 50°C, 75°C, and 100°C. The weight change of the specimens exposed at 50°C shows that the weight increased with exposure time, due to absorbing a portion of oil. The weight increased sharply in
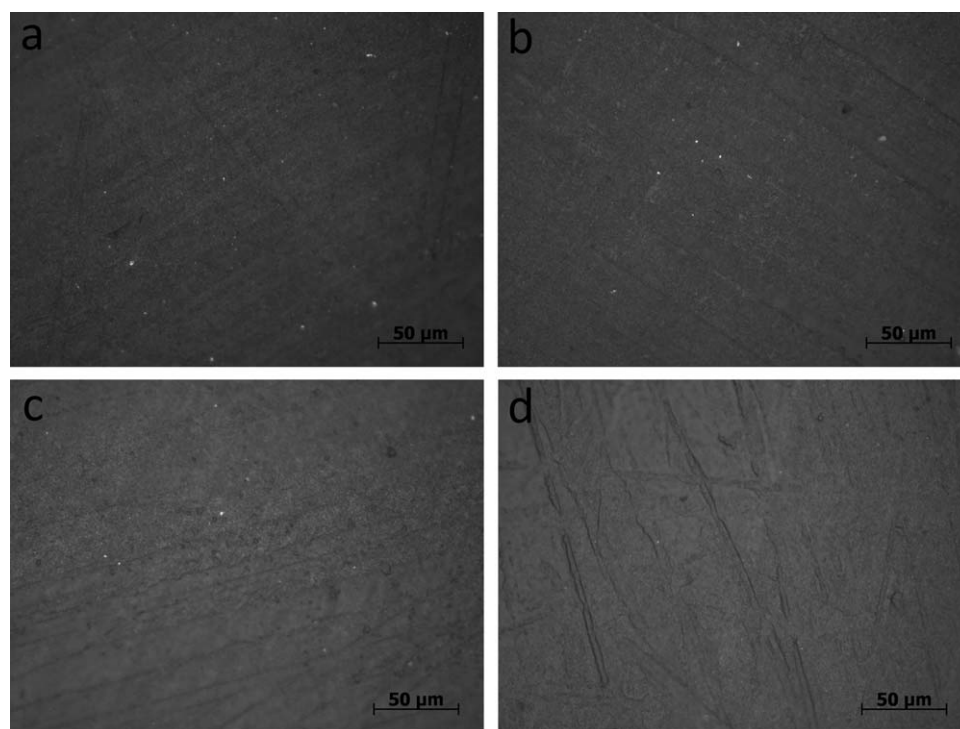
Figure 4. Topographical photos of the surfaces from the specimens in the crude oil: (a) before exposure, (b) after 8 weeks at 50 °C, (c) after 8 weeks at 75 °C and (d) after 8 weeks at 100 °C.

the first week and slightly in the other weeks. The specimens exposed at 75 °C show similar behavior, but with a variation depending on increased weight magnitude. The weight increase of the specimen at 75 °C was larger than that at 50 °C at identical exposure times, indicating that the temperature could accelerate the crude oil absorption. The specimens exposed at 100 °C show a clear difference in the weight increase rate. The weight increase rate of the specimen at 100 °C was the fastest in the first 3 days, but the weight increase rate became the slowest after 3 days of exposure. A possible explanation for this behavior is that the crude oil absorbs quickly into the HNBR material in the early stages of exposure, but the increasing crosslink density due to material degradation over time prevents the crude oil from further absorption.

Overall, it is concluded from this study that temperature has a significant effect on the weight increase: the HNBR material has more weight increase at higher temperature in the early stages of exposure, and the effect due to increasing crosslink density only obviously appeared at 100 °C.

Microscopy
The topographical changes on the surfaces of the specimens before exposure and after 8 weeks of exposure to the crude oil at 50 °C, 75 °C, and 100 °C were obtained by optical microscopy, as shown in Figure 4. The magnification is 500×. Figure 4(a) presents the surface micrograph of the specimen before exposure. It can be seen in Figure 4(a) that there were slight holes and channels in the specimen surface.

Figure 4(b) presents the surface microtopography changes of the HNBR material after exposure to the crude oil at 50 °C for

8 weeks. It can be found that the channels changed little, but larger holes appeared in the surface. The holes were caused by the crude oil. This result indicates that some additives or HNBR could dissolve in the crude oil.

Figure 4(c) shows the surface micromorphology changes of the specimens after exposure to the crude oil at 75 °C for 8 weeks. It can be seen from Figure 4(c) that the surface of the specimen became rougher. Compared to the specimen after 8 weeks of exposure at 50 °C, the deeper channels in the surfaces could be clearly observed, and the number of the larger holes increased for the specimen after 8 weeks of exposure at 75 °C.

Figure 4(d) shows the typical surface condition of the HNBR material after exposure to the crude oil at 100 °C for 8 weeks. The surface of the specimen after 8 weeks of exposure at 100 °C was roughest among those at 50 °C, 75 °C, and 100 °C. The channels in Figure 4(d) were deeper and wider than those in the other specimens, which results from the growing of holes. The holes may become part of the channels and cannot be observed, obviously.

It can be concluded that the surface damage of the HNBR specimens at higher aging temperature is more severe, and the degradation is characterized by the growing of the holes and channels on the surfaces, exhibiting the effects of the crude oil and temperature.

ATR-FTIR Analysis
The aim of the ATR-FTIR analysis is to determine the chemical changes of the HNBR material aged by crude oil at different aging temperatures. The comparison of the ATR-FTIR absorption spectra of specimens before and after exposure to the crude
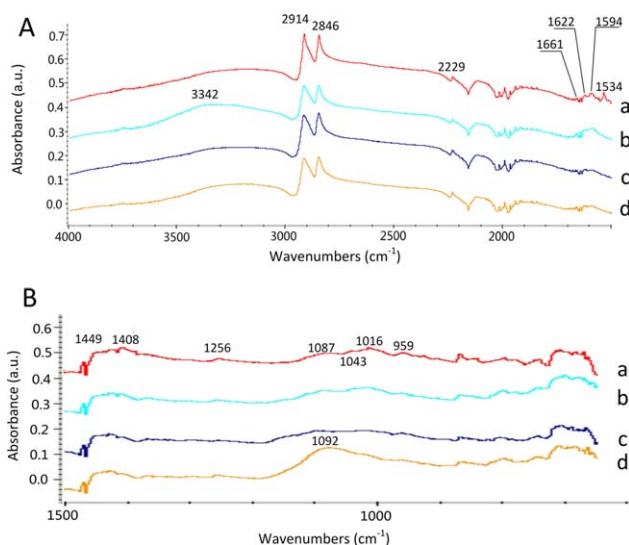
Figure 5. Comparison of ATR-FTIR results for the specimens in crude oil after 8 weeks of exposure: (A) spectra from 1500 to 4000 cm^{-1}, (B) spectra from 650 to 1500 cm^{-1}; (a) without exposure, (b) at 50 °C, (c) at 75 °C, and (d) at 100 °C. [Color figure can be viewed in the online issue, which is available at wileyonlinelibrary.com.]

oil was performed at various aging temperatures, as shown in Figure 5. Figure 5 shows the ATR-FTIR results before and after 8 weeks of exposure at 50 °C, 75 °C, and 100 °C, respectively.

Curve (a) in Figure 5 represents the HNBR material before exposure. It can be seen that the broadest band between 3500 cm^{-1} and 2200 cm^{-1} is observed and can be attributed to the O—H bond stretching vibrations in the alcohol group influenced by the —NH$_2$ group, so other peaks at 3500–3000 cm^{-1} cannot be observed. The C—O stretching vibration for the alcohol group is at 1016 cm^{-1} and 1043 cm^{-1}. The peaks at 1594 cm^{-1} and 1087 cm^{-1} demonstrate the presence of the NH$_2$ group in the rubber material. The peaks at 1594 cm^{-1} and 1087 cm^{-1} result from the N—H deformation vibration and C—N deformation vibration in the NH$_2$ group. The peaks at 2914 cm^{-1}, 2846 cm^{-1}, and 1449 cm^{-1} can be attributed to the C—H stretching vibrations and the C—H blend vibration in the CH$_2$ group. The absorption peak of the C≡N stretching vibration is at 2229 cm^{-1}. The absorbance of the C—H deformation vibration for 1,4-*trans*-vinylene is at 959 cm^{-1}. The peaks at 1431 cm^{-1} can be attributed to the C—H bond bending vibration of CH$_3$. The absorptions between 2200 cm^{-1} and 2000 cm^{-1} may result from the double bond vibrations of N=C=S, which may exist in the additives. The absorption peaks at 1661 cm^{-1}, 1622 cm^{-1}, and 1408 cm^{-1} indicate the presence of R—CO—NH$_2$ in the initial specimen. The C=O stretching vibration is at 1661 cm^{-1}, the N—H deformation vibration is at 1622 cm^{-1}, and the C—N stretching vibration is at 1408 cm^{-1}. In addition, the strong peak at 1408 cm^{-1} can also be attributed to the O—H deformation vibration of the additive (stearic acid). The C=O stretching vibration at 1640 cm^{-1}, the N—H deformation vibration at 1534 cm^{-1}, and the C—N stretching vibration at 1256 cm^{-1} imply the presence of R-CO-NH-R'.
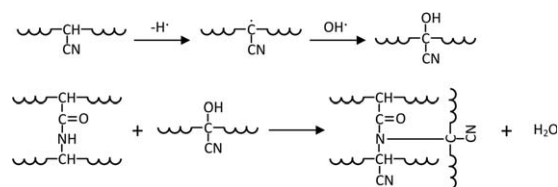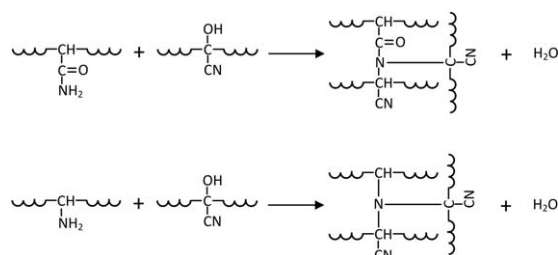

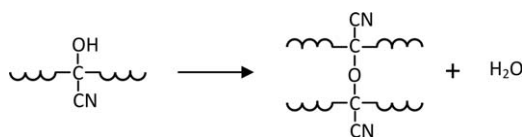**Scheme 1.** Reaction mechanism of HNBR material in crude oil at 50 °C.

Curve (b) in Figure 5 represents the HNBR material after 8 weeks of exposure at 50 °C. It can be found that a new strong absorption at 3342 cm^{-1} appeared and is assigned to the O—H bond for the alcohol group, suggesting that the radical reaction of the alcohol group appears in the surface of the HNBR material. The new alcohol group may be from the crude oil. The disappearance of the peak at 1534 cm^{-1} implies that the R-CO-NH-R' could have dissolved in the crude oil or has been converted into R-CO-N(-R')$_2$. In addition, the obvious decrease of the peak at 1408 cm^{-1} could be due to the stearic acid dissolving in the crude oil. The scheme of the main reaction at 50 °C is described as shown in Scheme 1.

Curve (c) in Figure 5 represents the HNBR material after 8 weeks of exposure at 75 °C. It can be found that, the same as for the phenomenon at 50 °C, the disappearance of the peak at 1534 cm^{-1} implies that the R-CO-NH-R' may have dissolved in the crude oil or has been converted into R-CO-N(-R')$_2$, as shown in Scheme 1. In addition, the decrease in the peaks at 1594 cm^{-1} and 1087 cm^{-1} indicates that there is a radical reaction for the NH$_2$ group when the aging temperature is raised to 75 °C. At the same time, the decrease of the peak at 1622 cm^{-1} and the disappearance of the peak at 1408 cm^{-1} are attributed to the chemical modification of the NH$_2$ group in the amide group. The C—O stretching vibration for the alcohol group at 1024 cm^{-1} decreases, indicating that the OH group partly reacts during the aging progress. Therefore, the decrease of the OH group and the NH$_2$ group leads to the primary amino group in the surface of the HNBR material converting into a tertiary amine group. The new reactions that appeared at 75 °C are shown in Scheme 2.

Curve (d) in Figure 5 represents the HNBR material after 8 weeks of exposure at 50 °C. It can be found that, the same as for the phenomenon at 50 °C, the disappearance of the peak at 1534 cm^{-1} implies that the R-CO-NH-R' may have dissolved in the crude oil or has been converted into R-CO-N(-R')$_2$, as shown in Scheme 1. And the same is true with the phenomenon at 75 °C: the decrease of the peaks at 1594 cm^{-1} and 1622 cm^{-1} indicates that there is also a radical reaction for the NH$_2$ group

Scheme 2. Reaction mechanism of HNBR material in crude oil at 75 °C.

Scheme 3. Reaction mechanism of HNBR material in crude oil at 100 °C.

and the NH_2 group in the amide group when the aging temperature is raised to 100 °C, as shown in Scheme 2. In addition, a strong broad peak at 1092 cm^{-1} appeared and can be attributed to R-O-R′; that is to say a new crosslinking reaction appeared at 100 °C. The new reaction that appeared at 100 °C is shown in Scheme 3.

The ATR-FTIR results indicate that the degradation mechanisms of the HNBR material after exposure to the crude oil could proceed via chemical crosslinking, and the reactions are different at the three temperatures. Therefore, the temperature and the crude oil have a direct effect on the chemical changes of the HNBR material.

Mechanical Property Test Results

Tensile Test. The selected representative tensile stress–strain curves for the specimens before and after exposure at different temperatures are shown in Figure 6.

Figure 6(a) shows the tensile stress–strain curves measured at 50 °C for the specimens before and after exposure at 50 °C. The tensile strength decreased sharply in the first week, and then the tensile strength changed little over the next 7 weeks. In addition, the tensile stiffness in the first 2 weeks decreased markedly compared to the stress in the other weeks. A large decrease of

the tensile elongation was also noted for the specimens after 1 week of exposure compared to the specimens before exposure, and the elongation increased slightly over the next 7 weeks. The results at 50 °C for the tensile tests markedly changed in the first week and changed little in the next weeks, similar to the weight change. This behavior indicates the effect of the crude oil. The sharp decrease for the elongation in the first week was caused by the crude oil and could be partially caused by the presence of holes and channels in the surface (see Figure 4) of the specimens after exposure. The elongation slightly increased in the next 7 weeks mainly because the absorbed crude oil worked by embedding itself between the chains of the specimen, decreasing the intermolecular attraction and increasing the mobility of the chains and thus improving the elongation for the HNBR material and making it softer.

Figure 6(b) presents the tensile stress–strain curves measured at 75 °C for the specimens before and after exposure at 75 °C. The tensile strength for the specimens after exposure at 75 °C had a behavior similar to that at 50 °C. For the stress–strain curves of the specimens after exposure, when the strain was less than about 40%, the stress was lower than that for the specimens before exposure. When the strain was more than about 40%, the stress was higher than that for the specimens before exposure. Moreover, the tensile elongation decreased sharply in the first week and decreased slightly in the other weeks. These behaviors indicate the crude oil played a main role in the specimens in the low-strain region, and temperature played a direct role in the specimens in the large-strain region. The crude oil embedded itself between the chains of the specimen to make
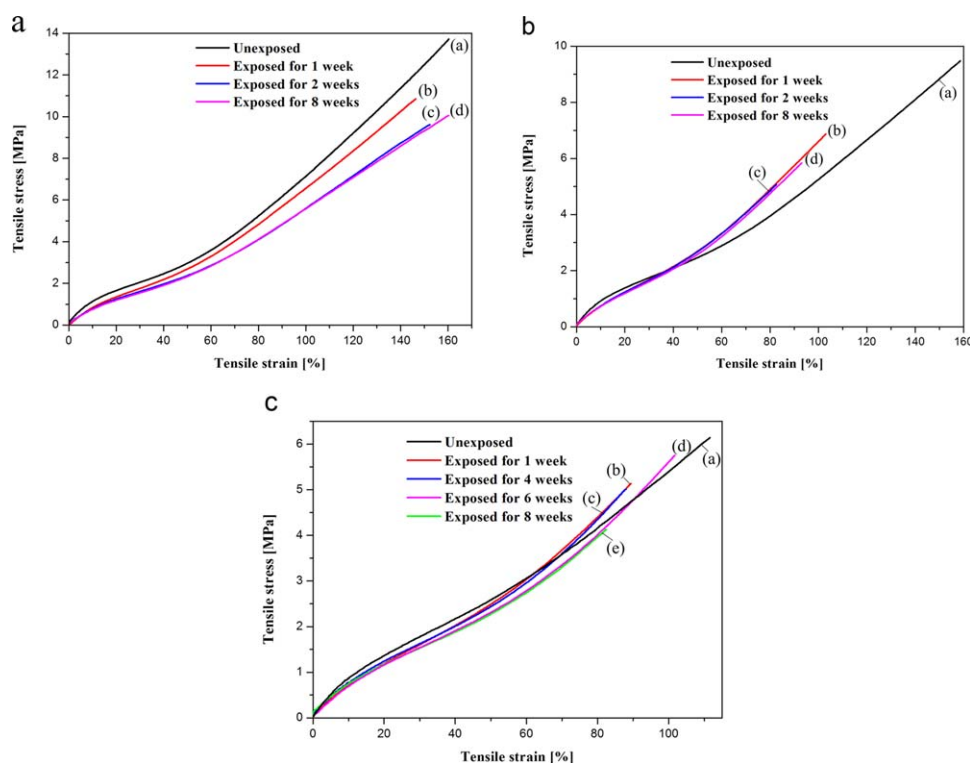

Figure 6. Tensile stress–strain curves of the specimens before and after exposure to crude oil: (a) exposed and measured at 50 °C, (b) exposed and measured at 75 °C, and (c) exposed and measured at 100 °C. [Color figure can be viewed in the online issue, which is available at wileyonlinelibrary.com.]
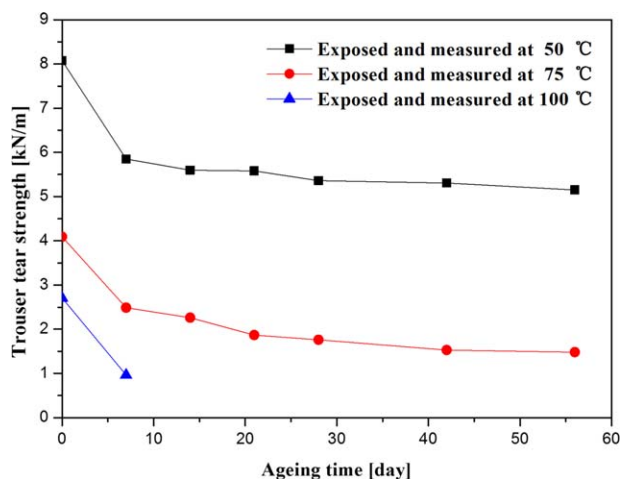
Figure 7. Trouser tear strength for the HNBR material after exposure to crude oil at 50 °C, 75 °C and 100 °C varying with time. [Color figure can be viewed in the online issue, which is available at wileyonlinelibrary.com.]

Figure 9. Compressive moduli at 25% of the HNBR specimens after exposure to crude oil at 50 °C, 75 °C, and 100 °C varying with time. [Color figure can be viewed in the online issue, which is available at wileyonlinelibrary.com.]

the specimens softer. The temperature led to crosslinking (Scheme 2), making the tensile stiffness increase in the large-strain region. The elongation decrease was caused by the crude oil and might partially result from the presence of holes and channels (Figure 4) in the surface of the specimens after aging.

Figure 6(c) presents the tensile stress–strain curves measured at 100 °C for the specimens before and after exposure at 100 °C. The tensile strength for the specimens after exposure at 100 °C also had a behavior similar to that at 50 °C. Similar to the specimens at 75 °C, the specimens at 100 °C softened in the low-strain region and hardened in the large-strain region. In addition, the elongation at break decreased sharply in the first week and decreased slightly in the other weeks. However, the specimens after exposure at 100 °C show a difference in behavior, with the stress stiffness decreasing sharply in the first and the fifth weeks. The stress stiffness decreased more seriously than at 75 °C. This behavior implies that the degradation at 100 °C, including backbone scission, phase separation, and crosslink breaking, may have a greater impact on the HNBR material than that at 75 °C. These results indicate the temperature and crude oil effects.

Tear Test. The tear strength property varying with time under various temperatures is shown in Figure 7. In the figure, it can be found that the tear property of the HNBR material decreased with time at the three temperatures, especially in the first week, and the higher aging temperature led to a lower tear strength from 1 to 8 weeks.

Figure 8. Tested tear specimen after 8 weeks of exposure to crude oil at 100 °C. [Color figure can be viewed in the online issue, which is available at wileyonlinelibrary.com.]
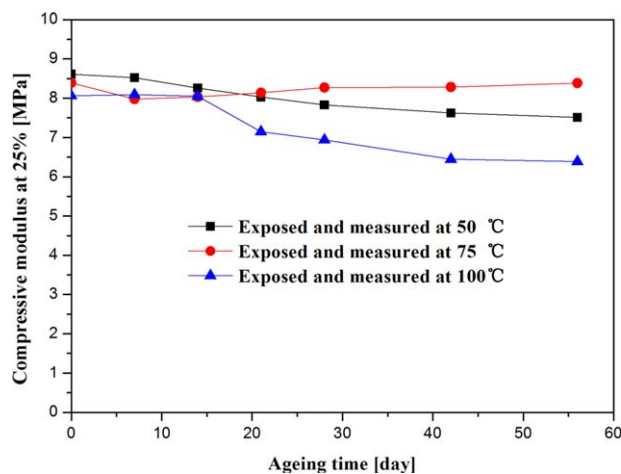
Note that the results from 2 weeks of exposure to the crude oil at the aging temperature of 100 °C for the HNBR material are not shown here because the length due to tear sharply decreased, and the number of peaks in the multipeak traces decreased, and especially after 8 weeks of exposure the lamellar rubber was peeled from the aged specimens (as shown in Figure 8). This behavior indicates the presence of backbone scission, phase separation, and crosslink breaking in the specimens after exposure at 100 °C.

Compressive Stress–Strain Test. Figure 9 shows the compressive moduli at 25% for the specimens under different temperatures. The compressive properties at the various temperatures show the same behavior as for the tensile properties. As expected, the compression modulus decreased with time at 50 °C and 100 °C. Moreover, the compression modulus at 25% decreased sharply in the first week and then increased slightly with aging time at 75 °C.

Figure 10 shows the selected representative uniaxial compressive stress–strain curves for the HNBR material specimens before exposure and after exposure to the crude oil at 50 °C, 75 °C, and 100 °C. The compressive stress–strain curve contains the loading curve and the unloading curve. Hysteresis is a particular characteristic in elastomers. It represents the loss of energy and overheating.[29] The rate of hysteresis can be calculated from the compressive stress–strain curves. The area below the loading curve corresponds to the energy applied in the loading stage, and the area below the unloading curve corresponds to energy recovered. The area between the two curves represents the energy lost from the hysteresis. Figure 11 shows the ratios between the hysteresis energy and the loading energy for the HNBR specimens after exposure to the crude oil at 50 °C, 75 °C, and 100 °C varying with time. It can be seen that the energy changed substantially after exposure to the aging environments over time. Both the crude oil and the aging temperature had a significant effect on the loss energy in the identical test conditions. The loss energy percent for the unexposed specimens
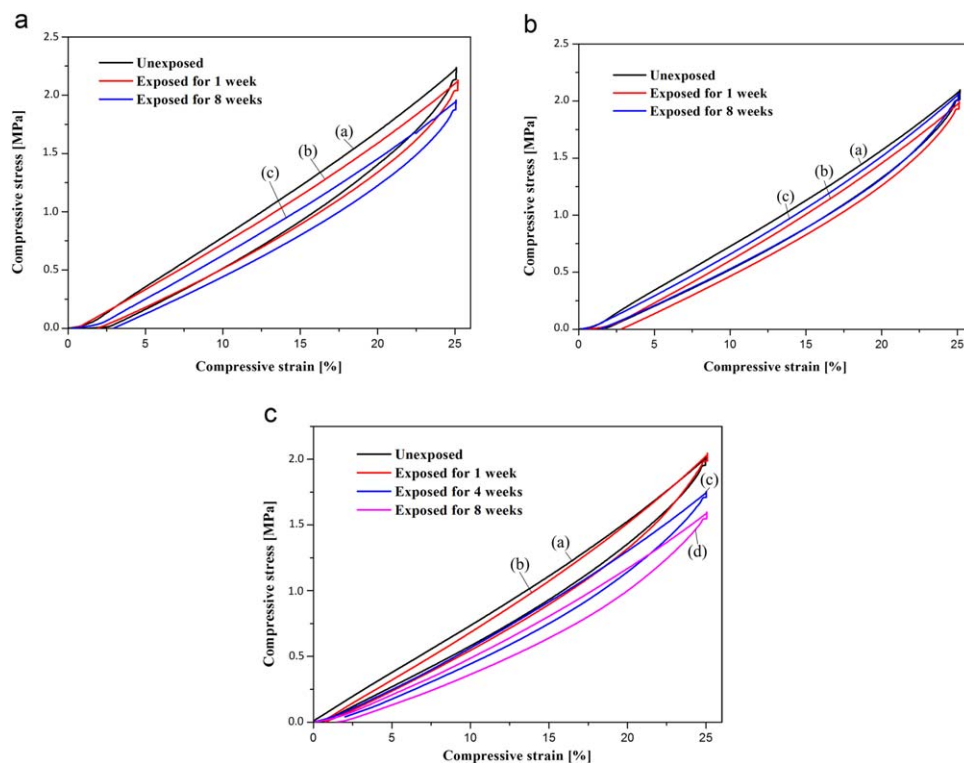
Figure 10. Compressive stress–strain curves of the HNBR specimens after exposure to crude oil varying with time: (a) exposed and measured at 50 °C, (b) exposed and measured at 75 °C and (c) exposed and measured at 100°C. [Color figure can be viewed in the online issue, which is available at wileyonlinelibrary.com.]

decreased with aging temperature. Besides, the loss energy percent decreased first and then changed little from the first week at 50 °C, increased from the third week at 75 °C, and increased from the second week at 100 °C. It is noted that hysteresis is caused by the viscoelastic nature of the polymer. Therefore, the change of the loss energy from our test indicates that the viscoelastic property of the material has been changed after exposure to the crude oil environment.
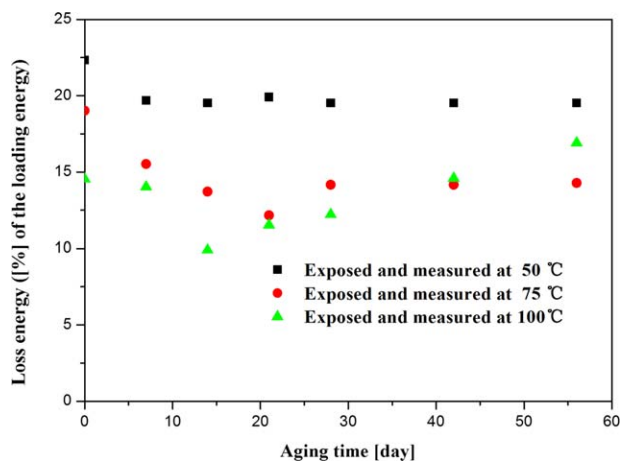
Compression Set Test. The compression set rate over time at the different aging temperatures for the HNBR specimens before and after exposure is shown in Figure 12. It can be found that the compression set rate of the specimens after 1 week of exposure became smaller at 50 °C and 75 °C than that of the specimens before exposure, and the compression set at 100 °C became larger after 1 week of exposure. These behaviors indicate that the temperature and crude oil had a significant effect on the variation of the compression set. The decrease of the
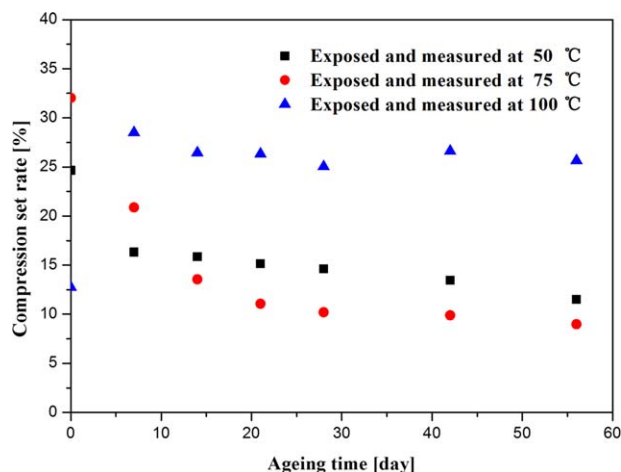

Figure 11. Ratios between the hysteresis energy and the loading energy for the HNBR specimens after exposure to crude oil at 50 °C, 75 °C and 100 °C varying with time. [Color figure can be viewed in the online issue, which is available at wileyonlinelibrary.com.]

Figure 12. Compression set rates of the HNBR specimens after exposure to crude oil at 50 °C, 75 °C and 100 °C varying with time. [Color figure can be viewed in the online issue, which is available at wileyonlinelibrary.com.]

compression set rate at 50 °C and 75 °C indicates that the crude oil had a beneficial effect on the compression set property. In addition, the compression set rate for the specimen after 1 week exposure at 75 °C decreased sharply, indicating that the crosslinking also played an important role at 75 °C. Conversely, the increase of the compression set rate in the first week at 100 °C was sharp, which implies that the degradation had a greater impact on the HNBR material at 100 °C than at 50 °C and 75 °C.

CONCLUSIONS

The degradation processes of HNBR material were investigated in a crude oil environment at the aging temperatures of 50 °C, 75 °C, and 100 °C. The following conclusions can be made:

1. Temperature has a significant effect on the weight change: the HNBR material has a greater weight increase at higher temperature in the early stages of exposure, and the effect due to increasing crosslink density only obviously appeared at 100 °C.
2. The optical microscopy results show that the surface damage of the HNBR specimens at higher exposure temperature is more severe, and the degradation is characterized by the growing of holes and channels on the surfaces, exhibiting the effects of the crude oil and temperature.
3. The ATR-FTIR results reveal that the degradation mechanisms of the HNBR material after exposure to the crude oil could proceed via chemical crosslinking, and the higher temperature could lead to increasing crosslink density. The results indicate the temperature and the crude oil have the direct effect on the chemical changes of the HNBR material.
4. The physical and mechanical test results show that the properties of the HNBR material change significantly after exposure. The results imply that the presence of chain mobility in the aging process and the degradation due to backbone scission, phase separation, and crosslink breaking have a greater impact on the HNBR material at 100 °C than at 50 °C and 75 °C.
5. The current work shows the degradation mechanisms and the degradation in the physical–mechanical properties in the HNBR material in a simulated crude oil environment. The chemical and mechanical degradation may affect the stability and durability of the HNBR material in the stress relaxation behavior and dynamic mechanical properties. The effect of degradation on the stress relaxation behavior and dynamic mechanical properties of the HNBR material after exposure to the crude oil at various temperatures is under investigation and will be reported later.

REFERENCES

1. Manoj, N.; De, P. *Polym. Degrad. Stabil.* **1994**, *44*, 43.
2. Perraud, S.; Vallat, M.-F.; David, M.-O.; Kuczynski, J. *Polym. Degrad. Stab.* **2010**, *95*, 1495.
3. Guo, F.; Jia, X. H.; Lv, M. D.; Wang, L. K.; Salant, R. F.; Wang, Y. M. *Tribol. Int.* **2014**, *78*, 187.
4. Pan, L.; Tan, J. *J. Petrol. Sci. Eng.* **2015**, *134*, 176.
5. Dato, J. E.; Campomizzi, E. C.; Achten, D. *Rubber World* **2007**, *236*, 28.
6. Wrana, C.; Reinartz, K.; Winkelbach, H. R. *Macromol. Mater. Eng. 286*, 657, **2001**.
7. Mousa, A.; Ishiaku, U. S.; Mohd Ishak, Z. A. *Polym. Bull.* **2005**, *53*, 203.
8. Sirisinha, C.; Sae-Oui, P.; Guaysomboon, J. *J. Appl. Polym. Sci.* **2002**, *84*, 22.
9. Sae-Oui, P.; Sirisinha, C.; Wantana, T.; Hatthapanit, K. *J. Appl. Polym. Sci.* **2007**, *104*, 3478.
10. Sirisinha, C.; Saeoui, P.; Guaysomboon, J. *Polymer* **2004**, *45*, 4909.
11. Dinzburg, B. N.; Gillen, K. T. *Lubr. Eng.* **2002**, *58*, 21.
12. Jennewein, B.; Frolich, D. In Proceedings of the 17th International Sealing Conference; Stuttgart, Germany, **2012**; p 526.
13. Denardin, E. L. G.; Janissek, P. R.; Samios, D. *Thermochim. Acta.* **2002**, *395*, 159.
14. Shaaban, A.; Se, S.-M.; Dimin, M. F.; Juoi, J. M.; Mohd Husin, M. H.; Mitan, N. M. M. *J. Anal. Appl. Pyrol.* **2014**, *107*, 31.
15. Rey, T.; Chagnon, G.; Le Cam, J. B.; Favier, D. *Polym. Test.* **2013**, *32*, 492.
16. Chou, H.-W.; Huang, J.-S.; Lin, S.-T. *J. Appl. Polym. Sci.* **2007**, *103*, 1244.
17. Chou, H.-W.; Huang, J.-S. *J. Appl. Polym. Sci.* **2008**, *107*, 1635.
18. Cadambi, R. M.; Ghassemieh, E. *J. Elastomers Plast.* **2012**, *44*, 353.
19. Wang, T. T.; Zhong, G. L.; Zhou, L. L. *Adv. Mater. Res.* **2013**, *750–752*, 816.
20. Nasreddine, V.; Kulbaba, K.; David, S. *Rubber World* **2013**, *248*, 32.
21. Sheng, C. R.; Hu, Z. W.; Martin, H.; Duan, Y. X.; Zhang, J. M. *J. Appl. Polym. Sci.* **2015**, *132*, 41612.
22. Alcock, B.; Jørgensen, J. K. *Polym. Test.* **2015**, *46*, 50.
23. Bender, H.; Campomizzi, E. *KGK, Kautsch. Gummi Kunstst.* **2001**, *54*, 14.
24. Chaudhry, R. A.; Hussein, I. A.; Amin, M. B.; Abu Sharkh, B. F. *J. Appl. Polym. Sci.* **2005**, *97*, 1432.
25. Chen, S.; Yu, H.; Ren, W.; Zhang, Y. *Thermochim. Acta.* **2009**, *491*, 103.
26. Smith, K. C.; Tripathy, B. S. *Rubber World* **1998**, *217*, 28.
27. Cong, C.-B.; Cui, C.-C.; Meng, X.-Y.; Lu, S.-J.; Zhou, Q. *Chem. Res. Chin. Univ.* **2013**, *29*, 806.
28. Choudhury, A.; Bhowmick, A. K.; Soddemann, M. *Polym. Degrad. Stab.* **2010**, *95*, 2555.
29. Tan, J.; Chao, Y. J.; Li, X.; Van Zee, J. W. *J. Fuel Cell Sci. Tech.* **2009**, *6*, 1.